MAPPING THE MIND

Visualizing Cortico-Cortical Evoked Potentials to Explore Functional Connectivity

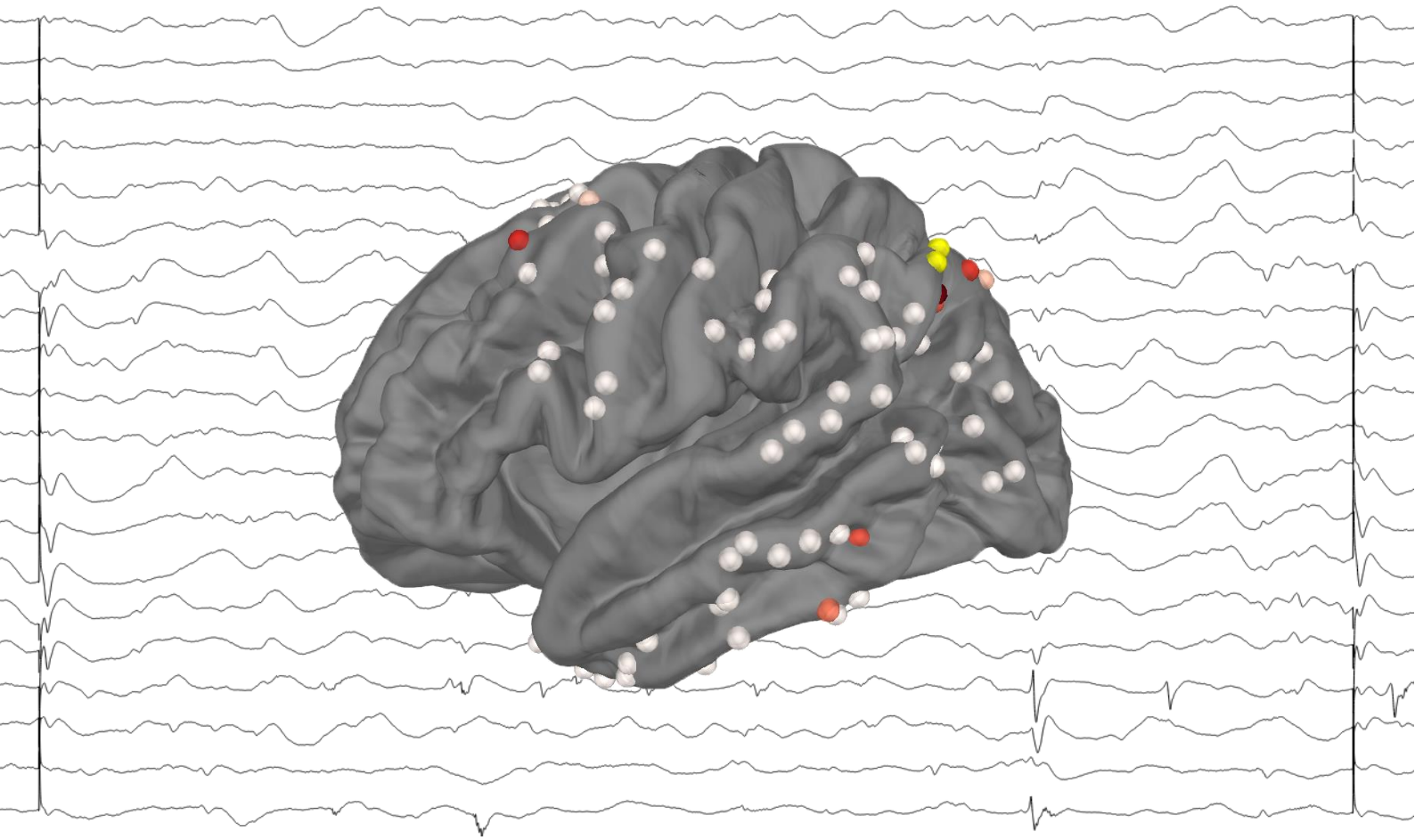

J.J.B. Teurlings

Department of Neurology – Clinical Neurophysiology
Department of Neuroscience
Erasmus Medical Center, Rotterdam
August 2024

MAPPING THE MIND

Visualizing Cortico-Cortical Evoked Potentials to Explore Functional Connectivity

Jeroen Teurlings
Student number : 4672429
August 19, 2024

Thesis in partial fulfilment of the requirements for the joint degree of

Master of Science

in Technical Medicine

Leiden University; Delft University of Technology; Erasmus University Rotterdam

Master thesis project (TM30004; 35 ECTS)
Department of Neurology – Clinical Neurophysiology
Department of Neuroscience
Erasmus MC
January 22, 2024 – August 19, 2024

Supervisors:

Dr. R. (Robert) van den Berg	Medical supervision
Dr. Z. (Zhenyu) Gao, Associate Professor	Technical supervision

Thesis committee members:

Dr. Z. (Zhenyu) Gao, Associate Professor	Erasmus MC	Chair
Dr. R. (Robert) van den Berg	Erasmus MC	
Dr. Ir. P (Pieter) Kruizinga	TU Delft, Erasmus MC	

Universiteit Leiden
TU Delft Delft University of Technology
Erasmus Universiteit Rotterdam

Preface

This very first page is the last page I write and also marks the end of my time as a student. What started as doubting between medicine or something more technical to study 7 years ago, and not really knowing what I was doing or wanted to become, ended in this thesis and knowing just a little bit more. Throughout my student time I've always said that I wanted to work in a neuro-oriented field. It has guided every choice up until now, from choosing a minor, choosing a track, and finally starting my master's thesis. Starting from the third clinical internship in the second year of the master, I focusses mainly on neurology, neurosurgery, neuroscience and mostly anything that had a slight connection to the brain. This mysterious organ intrigues me more than anything and I get excited every time I think about how much we still have to learn. With this thesis I wanted to create new knowledge that could be used to understand our brain and use it for making us better and more healthy humans. Throughout my thesis I introduced myself to the world of Brain Computer Interfaces, Neuromorphic Engineering, and Brain Connectomics. I hope I can use this thesis as a stepping stone to a career in this field, as I find it endlessly intriguing and future-worthy.

I want to thank my supervisors, Robert and Gao, for assisting me throughout this project. Robert, thank you for always being enthusiastic about the project going forward and given me so much of your precious time. Hopefully I have given you something in return for one of your many interesting projects in your very own AI-lab. Thank you for allowing me to have wild ideas and pursue them, but also tell me straight up when those wouldn't work. I think we have discussed many different ways how this project could come to an end, but I'm happy with the result. Gao, we did not have many meetings, but when we did, it were some of the most productive and fruitful meetings I've had. Thank you for giving me many new insights throughout the project and always taking the time to listen what Robert and I came up with, even with your very busy calendar.

I want to thank Dorien, for introducing me to the data that she gathered herself, on which practically all of this thesis is build. Our initial talk sparked much of the ideas for this work and gave me the head start I needed to get this project off the ground. I also want to thank all the other Technical Medicine students who allowed me to think about other projects than just my own and broadened my vision to more than just electrodes on a brain. I enjoyed our weekly meeting where I could always show some new visualization that I fabricated. I appreciate all the feedback and motivation you gave me when I thought nothing was going to work.

Lastly, I want to thank my friends for the countless lunch walks during this project and for sharing this adventure with me, my parents for always allowing me to follow my dreams without any worries, and especially Karo, for her relentless support and happy sunshine nature. You are my ray of light and I cannot express how much I appreciate everything you do for me each day. I hope you will forgive me for that.

To the readers of this thesis, thank you for your time and I hope I can transfer some of my enthusiasm on this subject through these pages.

Jeroen Teurlings

August 2024

Summary

The brain is one of the most important organs of the human body, yet it remains poorly understood. The anatomical connections between different brain regions facilitate the transmission of electrical signals across the brain, forming the basis of higher functionalities such as speech, vision, comprehension, and sensory perception. During brain tumor surgery, it is critical to preserve vital connections within the brain while resecting as much of the tumor as possible. Therefore, accurately locating and mapping functional tracts within the brain is crucial for optimal patient outcomes. This thesis focuses on the exploration and application of electrocorticography (ECoG) and Cortico-Cortical Evoked Potentials (CCEP) to enhance our understanding of brain connectivity to ultimately aid in the improvement of tumor resection.

The **Background** chapter provides all necessary information on the electrophysiological brain, intraoperative neuromonitoring, ECoG, and CCEP. By explaining the fundamental concepts and technological aspects, the chapter sets the stage for understanding how ECoG and CCEP can be utilized to study brain connectivity and improve surgical outcomes.

Chapter 1 establishes the foundation of the study. It uses data from a study on brain transmission speeds involving 74 patients who underwent epilepsy surgery. The chapter explains the composition and structure of the raw data, explaining the processes of data loading and preprocessing, including the construction of epochs and evoked objects from the raw data. The peak detection algorithm, the primary analysis method used to extract amplitude and latency parameters from registered CCEP N1 peaks, is illustrated. These results, a combination of the CCEP connections between electrodes and their corresponding amplitude and latency, form the basis for further chapters.

In **Chapter 2**, the study primarily addresses the analysis of CCEP responses measured with ECoG across a population. The analysis made a construction of brain connectivity graphs based on Destrieux labels and individual electrodes. The peak detection algorithm identified various CCEP responses and highlighted connections between stimulating and recording electrodes. Notably, connections between temporal and parietal brain regions, and between parietal and frontal regions, were found. These findings corresponded with known white matter tracts, demonstrating the capability of CCEP measurements to reflect connectivity, comparable to standard Diffusor Tensor Imaging (DTI) measurements.

Chapter 3 shifts the focus to the visualization of these CCEP responses at an individual patient level for clinical translation. Stimulation of electrodes in the parietal region revealed both local responses and distant connections in the frontal and temporal regions of an exemplary patient. These visualizations provide intuitive insights into the brain's connectivity. An animation illustrating the temporal progression of signal propagation offers a basis for personalized visualizations of connectivity based on CCEP measurements.

In summary, this work contributes to the field of neuroscience by providing robust methods for visualizing and analyzing brain connectivity, ultimately enhancing our ability to translate these findings into practical clinical applications.

Contents

Background

The Electrophysiological Brain

The brain is one of the most important organs in the human body, responsible for a plethora of functions and systems essential for life. It consists of billions of neurons structured to exchange information between the brain and the body. This complex transmission of information is vital for human survival. Acting as a command center, the brain controls all the processes of the body, with each region of the brain having its specific functionality. These functional areas are connected by white matter tracts, anatomical brain structures, which convey information between different brain regions. These anatomical connections lay the foundation for higher cognitive processes, enabling intelligent functions such as speech, vision, comprehension, and sensory perception, which combine the functionality of multiple brain regions [1, 2].

Neurons within the brain are connected via synapses, communicating and conveying information through rapid electrical signals known as action potentials. A complex system of ion channels propagates these action potentials across axons and dendrites, forming wire-like connections that transport signals throughout the brain and between the functional areas. The collective electric currents within a brain volume create a electric potential in the extracellular medium relative to a reference potential. This electrical activity of the brain encompasses all underlying processes and gives insight in the complex processes happening within [1, 2].

Since 1924, researchers have been measuring this electrical activity of the brain, leading to the development of electroencephalography (EEG) [3]. EEG measures potentials by placing electrodes on the scalp and comparing the recorded potentials with a reference electrode. The morphology of the recorded waveforms, including parameters like amplitude and frequency, is proportional to the multiple sources for electrical brain activity within a volume of brain tissue [2]. Recording these unique and complex waveforms provide researchers and clinicians valuable insights into brain processes, aiding in the diagnosis and treatment of disorders like epilepsy. However, despite these advancements, much of the brain's functionality remains poorly understood.

Intraoperative Neuromonitoring

Disturbances in physiological integrity of the brain, due to malignancy or epileptic brain tissue, can disrupt electrophysiological processes [4]. Maintaining the integrity and functionality of anatomical connections and white matter tracts is crucial for the brain to perform its tasks accurately and precisely. When these tracts or cortical areas are at risk of damage, intervention might be necessary to preserve brain functionality. Interventions for brain tumors can include radiation therapy, chemotherapy, targeted drug therapies, or surgery [5].

During brain tumor surgery, part of the patient's skull is removed and the brain tumor is resected. The extent of resection (EOR) of tumorous tissue strongly correlates with the patient's outcome [6, 7, 8]. Neurosurgeons aim for maximal safe resection, balancing the removal of tumorous tissue with the preservation of functional tissue to maintain the patient's quality of life after surgery.

To preserve as much functional tissue during surgery as possible, intra-operative neurophysiological monitoring (IONM) is often applied [9]. IONM includes all measurements performed during surgery to ensure the functionality of neurological systems. Examples of IONM include somatosensory evoked potentials (SSEP), motor evoked potentials (MEP), brainstem auditory evoked potentials (BAEP), visual evoked potentials (VEP), electromyography (EMG), EEG, and Electrocorticography (ECoG) [10]. The primary goal of IONM is to protect vital brain functions and prevent neurological damage. IONM serves two main purposes during surgery: monitoring existing signal transmissions and alerting neurosurgeons to deviations, and mapping brain regions and their functions [9].

Electrocorticography

The primary focus of this thesis will be ECoG measurements. ECoG is a collective name for recordings of electric potentials caused by brain activity which are taken directly from the cerebral cortex [6, 3]. ECoG allows for the intraoperative measurement and monitoring of brain activity, combining the flexibility of intraoperative measurements with the functionality of traditional EEG. In IONM, ECoG is often used alongside other monitoring techniques like functional magnetic resonance imaging (fMRI), transcranial motor evoked potentials (tMEP), and direct motor evoked potentials (dMEP)[11]. Once the skull is opened, ECoG provides the only way of directly measuring brain activity without penetrating the brain tissue, since EEG is no longer possible. Additionally, compared to EEG, ECoG has a higher density of electrodes per area, increasing the resolution of the measured signals. The technique has a higher signal-to-noise ratio (SNR), and higher spatial and temporal resolutions than traditional EEG[6]. This allows for a real-time, high-quality measurement of electric brain activity.

A typical ECoG setup consists of a sterile pad with integrated electrodes arranged in a grid. This grid enables direct cortical measurements, bypassing the skin and skull. Clinically, ECoG has greatly aided neurosurgeons and neurophysiologists in treating various neurological conditions. By providing real-time brain activity measurements, ECoG guides surgical interventions, allowing for more precise and targeted procedures [12]. It also helps localize critical brain areas, minimizing the risk of damaging essential functions during surgery [6]. Furthermore, ECoG has proven valuable in research, enhancing our understanding of brain functioning and the mechanisms underlying neurological disorders.

Cortico-Cortical Evoked Potentials

A novel technique that is tightly connected to ECoG is the measurement of cortico-cortical evoked potentials (CCEP), first documented by Matsumoto et al. (2004) [13]. With an ECoG grid in place, the neurosurgeon can stimulate specific brain regions with the electrodes of the grid. The evoked response to this stimulation can be recorded with the same grid and is called a CCEP. This technique enables the study of communication between different brain areas, providing crucial insights into the brain's connectivity and functional organization [14, 15]. The morphology of recorded CCEPs includes characteristics like latency and amplitudes. Typically, CCEPs exhibit distinct negative (N1, N2) and positive (P1, P2) deflections [15]. The N1 response, in particular, is considered a robust marker for the evoked potential, thought to be generated by synchronized, excitatory synaptic activation of layers of apical dendrites of pyramidal cells [2]. An example of a CCEP can be seen in Figure 1.

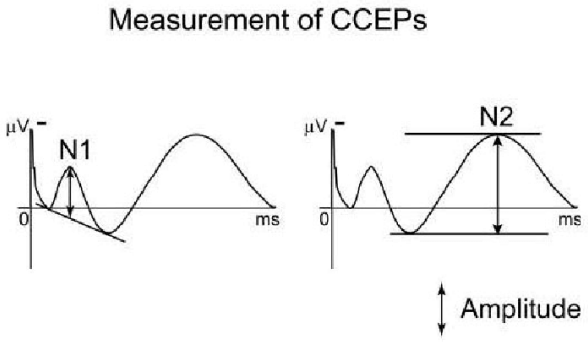

Figure 1: *Typical morphology of a CCEP response. CCEPs exhibit distinct negative (N1, N2) and positive (P1, P2. Not shown in figure) deflections. The N1 response is seen as the most robust marker for the CCEP response. This N1 peak has a latency (in milliseconds) and an amplitude (in microvolts) which can be used for further analysis. Adapted from Matsumoto et al. (2004) [13].*

Analyzing the latency and amplitudes of the N1 deflection provides valuable information about information processing within the brain. Combining ECoG with CCEPs allows researchers to explore connectivity between cortical areas and gain deeper insights into the brain's functional organization. Since the technique relies on the direct stimulation and recording of evoked potentials on the cortex,

it is inherently linked to the use of ECoG. During brain surgery, the registration of CCEPs can be used for both monitoring and mapping purposes [16, 17]. Monitoring can be done by checking if signal propagation remains intact during the procedure, alerting if any changes occur. Mapping of the cortex of the patient can be done by checking which parts of the brain are highly connected to other regions of the brain, which should then be avoided during resection.

Thesis Objective

Despite the increasing use and development of ECoG and CCEP registrations, these techniques are not yet routinely used in research or clinical practice at the Erasmus MC hospital. While there is interest in integrating ECoG measurements in the current IONM protocols, adequate knowledge and expertise is still lacking. CCEP measurements remain a research topic, with clinical translation yet to be achieved. This thesis aims to explore connectivity based on CCEP responses measured with ECoG to improve our scientific understanding of these signals, after which a clinical translation can be made by exploring fundamental methods for understanding CCEP signals in preparation for their implementation in future operating room (OR) settings. Efforts will focus on translating abstract signals into insightful visualizations, making clinical applications more feasible.

The main goals of this thesis are twofold:

- To explore connectivity within the human brain based on CCEP measurements performed with ECoG at a population level (**Chapter 2**).
- To visualize measured CCEP responses in a clear and intuitive way based on ECoG responses of individual patients (**Chapter 3**).

Results from this thesis should enhance the current understanding of electrophysiological connections within the brain and should lay the groundwork for further implementation of ECoG and CCEP registrations within the OR at Erasmus MC hospital.

CHAPTER 1

Data, Preprocessing, and Peak Detection

All code for this thesis was written in Python and a detailed description of the script is accessible via https://github.com/JeroenTeurlings/TM3_CCEP as comments and explanation within the code lines. The development of the script utilized GitHub CoPilot within MS Visual Studio Code, which provided AI-assisted coding support. The bulk of processing and visualization functionalities were built within the MNE environment, an open-source Python package for processing electrophysiological data [18].

1.1 Data

1.1.1 Data structure

The data used in this thesis was previously published in an openly accessible online repository by Van Blooijs et al. (2023) [19], which focused on the development of transmission speed in the human brain across different ages. This study utilized ECoG and CCEP measurements to calculate transmission speeds between known white matter tracts. The dataset, which is openly available online via https://openneuro.org/datasets/ds004080/, includes data from 74 patients (median age 17 years, range 4-51 years; 38 females) who underwent epilepsy surgery at the UMC Utrecht hospital between 2008 and 2020. All subjects who had single-pulse electrical stimulation (SPES) - a stimulation protocol where parts of the brain are stimulated with single pulses repeated ten times - for clinical purposes during the ECoG monitoring period from 2012 to 2020 were also included. Inclusion criteria were the absence of large brain lesions and the ability to determine electrode positions based on a CT scan co-registered with a T1 MRI scan. An overview of the included patients is shown in Table 1 in Supplementary Material A.

The dataset is organized according to the Brain Imaging Data Structure (BIDS) specifications, structured per patient, session, task, and run [20, 21]. Sessions denote the times of day when recordings took place, and tasks refer to specific measurements, in this case, SPES. Each run represents an individual measurement per patient, which can be repeated, resulting in multiple runs per patient.

For each run, data was saved according to the BrainVision Core data format (*BrainVision Core Brain Products GmbH, Gilching, Germany*), resulting in the following data files:

- **channels.tsv**: An overview of the included ECoG channels.
- **events.tsv**: Details of artifacts and stimulation times and characteristics.
- **electrodes.tsv**: Information on included electrodes, including quality measures, MRI 3D coordinates, and Destrieux labels.
- **.vhdr**: A text header file with metadata.
- **.vmrk**: A text marker file with event information.
- **.eeg**: A time-series file containing the raw ECoG data.

SPES was performed during ECoG recordings, with data sampled at 2,048 Hz using a MicroMed LTM64/128 express EEG headbox with an integrated programmable stimulator (*MicroMed, Mogliano Veneto, Italy*). Monophasic stimuli (10 pulses, 1 ms pulse width) were applied at a frequency of 0.2

Hz to two adjacent electrodes. Polarity was alternated after five pulses in 27 subjects to reduce stimulation artifacts. The current intensity was 8 mA, reduced to 4 mA near central nerves or the primary sensorimotor cortex to avoid pain or twitching.

1.1.2 Electrodes

ECoG data was recorded using subdural electrode grids and strips with a 4.2 mm^2 contact surface and 1 cm interelectrode distance. Additional depth electrodes were implanted in MRI-visible lesions, but were not included in this study. Electrode positions were determined via MRI scans and converted to Montreal Neurological Institute (MNI) 152 space (average brain coordinates produced by averaging brain MRI scans of 152 healthy individuals [22]) for easier reference and comparison. Electrodes were labeled according to the Destrieux atlas segmentation, an atlas that assigns labels to brain regions based on its anatomical position and functionality [23]. Overlapping electrodes, those on small structural abnormalities, or those with excessive noise were excluded from analyses. Stimulation pairs introducing baseline offsets were also excluded. In total, 6.3% of electrodes were excluded.

For a more detailed summary on the data structure, recording paradigms, or electrode specifics, refer to the article by Van Blooijs et al. (2023), "Developmental trajectory of transmission speed in the human brain"[19].

1.2 Preprocessing

1.2.1 Data Selection

Importing ECoG data that was saved according to the BrainVision format was done using basic MNE functions (mne.io.read_raw_brainvision). This read the header file (.vhdr) and automatically loaded the corresponding data files into an MNE-compatible structure. Additional data files (.tsv files including channel, electrode, and event data) were also loaded in.

Data was cleaned by selecting only ECoG channels and ignoring depth electrodes. Electrodes marked as "bad" due to overlap or excessive noise were excluded. This resulted in a cleaned dataset with high-quality ECoG channels. No additional filtering was applied beyond the internal Medtronic ADC filtering due to excellent signal quality, allowing for undisturbed CCEP analysis.

1.2.2 Events & Epochs

After refining the data, continuous data could be split into epochs. In MNE, 'epoch' objects show smaller time series around certain events. For this project, epochs of 4 seconds were created, centered around the stimulation event (t=0), resulting in time series 2 seconds before and 2 seconds after stimulation. Events were extracted from the 'events.tsv' file, which included the sample at which stimulation occurs and the electrode pair being stimulated. This creates epochs around every stimulation event, excluding steady-state ECoG data where no stimulation is performed. Each stimulation was repeated 10 times, and these could be averaged to create an 'evoked' class object, which represented the averaged response to 10 stimulations on one electrode pair. An example of a single evoked object is shown in Figure 1.1.

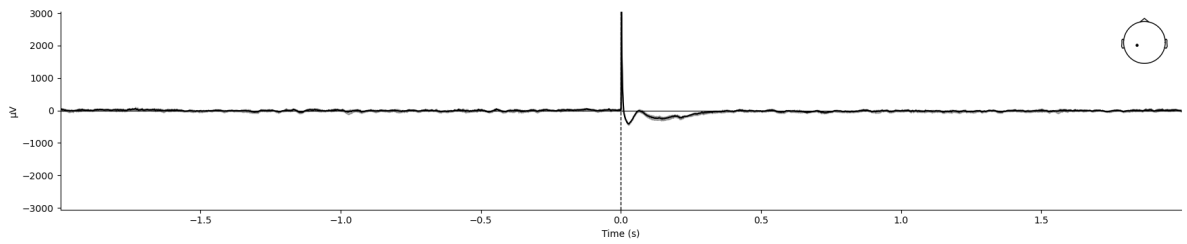

Figure 1.1: *Example of a single 'evoked' object showing the average epoch two seconds before and two seconds after stimulation. 10 Epochs were averaged into one evoked object, and the grey outline shows the variance between the 10 epochs. The representation of the head in the upper right corner shows the location of the recording electrode from which this registration was taken.*

Zooming in on the part of the signal around the stimulation moment, as can be seen in Figure 1.2, we can see in further detail what a CCEP response should look like. Just after stimulation on t=0, a big positive peak is present, which is the stimulus artefact that should be omitted from any analysis. The first negative deflection after this positive stimulus artefact is the N1 response of the CCEP, which can be used for further analysis.

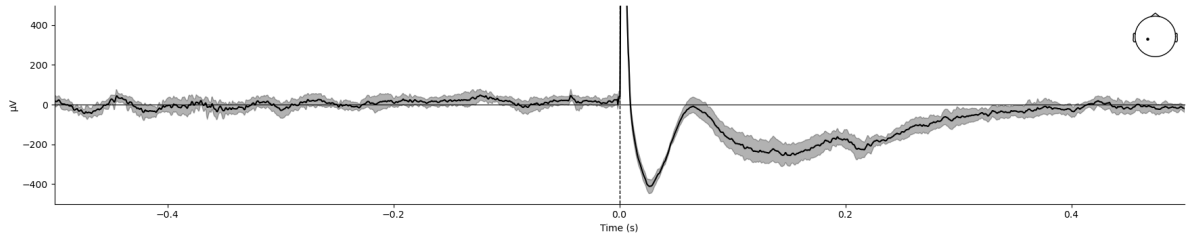

Figure 1.2: *Zoomed-in view of the single 'evoked' object from figure X, showing 0.5 seconds before and 0.5 seconds after stimulation. A distinct CCEP response can be seen, with a clear N1 peak. Note that the negative part of the signal is down, in contrast to the example given in Figure 1*

1.3 Peak Detection

A peak detection algorithm was developed to identify peaks in CCEPs following stimulation. Peak detection is crucial for CCEP analysis to find local maxima or minima, particularly the N1 peak, a key marker in CCEP literature. This first negative peak shows the cortex's initial response to external stimuli, providing amplitude and latency data for comparison between cortical areas. The peak detection algorithm was based on the algorithm used in the script that was developed for the article by Van Blooijs et al. (2023)[19]. The authors developed a peak detection algorithm that could accurately find the N1 peaks in the registered CCEP responses. This algorithm was originally made within MATLAB, but was translated to Python for this study.

Within Python, the Scipy Peak Detection function was used to scan for negative peaks in the signal between 0.009 and 0.1 seconds after stimulus. The first 9 milliseconds after stimulus were excluded from analysis to minimize the effect of the stimulus artefact, as advised by Van Blooijs et al. (2023)[19]. The algorithm used the following parameters:

- a minimum height of the peak based on 3.4x the pre-stimulus standard deviation of the signal from -2 to -0.1 seconds before stimulation
- a minimum standard deviation of 50 microvolts
- a minimum peak prominence of 20 microvolts

These values are used and tested by Van Blooijs et al. (2023)[19], and after testing within Python were also implemented here. Peaks were only detected if the local minimum of the signal complied with these parameters.

ECoG recordings varied between patients, which could disturb the peak detection algorithm. To make sure CCEPs were correctly registered, the peaks found by the peak detection algorithm were visually reviewed, and any incorrect detections were excluded. In total, 968428/2187338 (44.27%) of registered CCEPs were excluded. From the resulting, correct CCEP N1 peaks, the amplitudes and the latencies were extracted. Amplitude was defined as the height of the peak from baseline, and latency was defined as the time between the start of stimulation and the peak of the response. The use of the algorithm on the ECoG data per patient resulted in an amplitude and latency per CCEP peak and a list of electrodes that showed a connection based on CCEPs with corresponding Destrieux labels and Cartesian (i.e. xyz) coordinates. These values form the basis of upcoming CCEP analyses.

CHAPTER 2

Connectivity & Graph Analysis

2.1 Introduction

Expanding research into connected brain regions and their corresponding functions has given rise to a relatively new research field: Brain Connectomics [24]. This research into brain connectivity provides deeper insights into how the brain operates, functions, and forms connections. All brain tasks are based on networks and sequences of neuronal activity [25]. Brain connectomics offers a foundational field in neuroscience research, allowing us to investigate the underlying structural, functional, and effective networks to better understand the functionality of the brain and how specific actions come to be.

Within brain connectomics, three types of connectivity are distinguished[26]. Structural connectivity is based on anatomical contact between brain parts, focusing on the conduction pathways of synapses, neurons, white matter tracts, and other anatomical connections. Functional connectivity measures the temporal correlation of activity in various brain structures underlying neuronal activity, which relates to important functions like speech, memory, praxis, and emotions. The third connectivity level is effective connectivity, which is more complex and harder to visualize. Effective connectivity focuses on cause-and-effect relationships between brain regions, defining signal sources and receivers. Understanding these connections allows us to trace a specific signal from its source to its receiver and identify any changes along the way, providing significant insights into brain operations.

Each connectivity level has its modalities for visualization. Structural connectivity is primarily assessed using tractography and Diffusion Tensor Imaging (DTI), often used for presurgical planning to visualize white matter tracts beneath the brain's surface [27, 28]. This method extracts anatomical connections between cortex areas, suggesting connectivity based on these anatomical links. Functional connectivity is assessed with functional brain imaging technologies, including fMRI, EEG, and ECoG. fMRI, for example, measures the Blood Oxygen Level Dependent (BOLD) signal to investigate brain activity during specific tasks, revealing areas with increased blood flow and activity [29]. By comparing active areas, functional connectivity patterns can be identified. However, measuring or visualizing effective connectivity is more challenging [30]. CCEPs may provide a starting point for analyzing effective connectivity.

Analyzing CCEPs is a novel method for measuring brain connectivity and sheds light on connectivity within the brain [13]. By applying a current to the cortex (signal source) and measuring the response (signal receiver), we can gain further understanding on connectivity. Better understanding brain connectivity as a system could aid in treating diseases and disorders arising from network disturbances within the brain, such as epilepsy, migraines, and neuropathic pain.

Such a complex system can be analyzed using Graph Analytics, an emerging form of data analysis employing graph theory [31]. This method visualizes and analyzes data and connections within a graph to uncover complex relationships. Graph theory works with nodes (vertices) and edges (links between vertices), modeling pairwise interactions between objects. Therefore, it is a suitable analysis method for studying the network and connectivity within the brain's cortex since its activity is measured with electrodes, and links between electrodes.

In this chapter, we focus on brain connectivity. By viewing the brain as a system that can be analyzed using Graph Analytics, we aim to shed more light on brain connectomics in this patient population. We seek to demonstrate how CCEPs can visualize brain connectivity using graph theory as an alternative to fMRI, DTI, and EEG measurements, and compare the produced connections to known examples.

2.2 Methods

2.2.1 Data Preparation

From the peak detection algorithm described in Chapter 1, we obtained a list of CCEP responses for each patient, including amplitudes and latencies of the detected peaks. These responses indicated a connection between the positions of the stimulation electrode and the recording electrode, suggesting that these brain regions are connected.

For each connection, the Cartesian coordinates and linked Destrieux labels of both the stimulating and recording electrodes were extracted. Using the amplitude and latency data of the specific CCEP, a graph was constructed to visualize the various connections within the brain. In this graph, the electrodes (both stimulating and recording) were represented as nodes, and the connections between them (i.e., the CCEP responses) were represented as edges. Stimulated electrode pairs were seen as two individual electrodes being stimulated. So when one electrode pair generated a response in one other electrode, two edges would be created: one from both electrodes of the stimulation pair to the recording electrode.

The graph analysis was split into two parts: connections based on Destrieux labels and connections between individual electrodes.

2.2.2 Destrieux Label Analysis

All electrodes across all 74 patients with the same Destrieux label were grouped to analyze connected brain regions. This reduced the number of nodes to the number of used Destrieux labels. The strength of the connection was quantified with formula 2.1

$$weight = \frac{N_{CCEP}}{N_{stim}} * 100\% \tag{2.1}$$

Where N_{CCEP} is the total number of registered CCEPs, and N_{stim} is the total number of stimulations received by the Destrieux region. This percentage indicates the connection strength. Amplitude and latency were not included in this analysis due to the combination of multiple electrodes, making it difficult to analyze these parameters.

Nodes in the graph represented the average Cartesian coordinates of electrodes with the same Destrieux label. The coordinates of all electrodes with the same Destrieux label were averaged to produce a single 3D point per brain region. These points were considered nodes, and the connections between them were edges. The graph was constructed using NetworkX Python modules and plotted on a sample brain from BrainNet using Plotly Python modules. Edge thickness depended on the calculated weight, ranging from 0 (no connection) to 1 (strong connection).

2.2.3 Individual Electrode Analysis

The second analysis looked at connections found between individual electrodes of all 74 patients combined, without averaging them within brain regions. First, to gain a better understanding of the data being used, histograms of the distribution of edge length (the length of edges, the connection between two points) in millimeters, and the distribution of latency of the CCEP N1 peaks were plotted. Additionally, a scatterplot was made which showed the correlation between edge length and latency, exploring any underlying connection between the two parameters. Correlation was calculated with formula 2.2:

$$R_{ij} = \frac{C_{ij}}{\sqrt{C_{ii}C_{jj}}} \tag{2.2}$$

Where R is the correlation of two variables, and C is the covariance matrix of those variables. This formula was utilized by the numpy.corcoeff function in Python.

To produce the visualizations, individual electrodes were first plotted to ensure equal anatomical coverage per brain region. Here, nodes were defined as individual electrodes, and edges were again defined as CCEP connections. The distance between stimulation and recording electrodes was calculated using their respective Cartesian coordinates. To focus on distant connections, edges shorter than 80 millimeters were removed from the graph. With this minimal length the local responses between neighboring electrodes were expected to be excluded. Connection strength was visualized using the amplitude (thickness of the line) and latency (opacity of the line) of the recorded CCEPs.

2.2.4 Validation

The constructed graphs were compared with existing brain atlases and known anatomical connections for validation. Specifically, the ability to visualize cortical tracts with CCEP measurements was validated by comparing the results with existing visualizations of the same tracts. Using the article by Blooijs et al. (2023) [19], individual electrodes positioned on cortical endpoints of tracts were identified, and white matter tracts were visualized using DTI and tractography. These visualizations were compared to the graph analysis of individual electrodes (not Destrieux labels) to ensure consistency.

2.3 Results

2.3.1 Data Preparation and Initial Findings

The peak detection algorithm provided a comprehensive list of CCEP responses for each patient, detailing the amplitudes and latencies of detected peaks. These responses highlighted connections between the positions of the stimulating and recording electrodes, suggesting functional connectivity between these brain regions. The extracted Cartesian coordinates and linked Destrieux labels of both the stimulating and recording electrodes served as the foundation for constructing the brain connectivity graphs. Showing both the visualization of general CCEP connectivity based on Destrieux labels, and on individual electrodes, more insight into the brain its connectivity level was achieved.

Histograms of the distribution of edge length and latency is shown in figures 2.1 and 2.2. Here we can see a normally distributed, although skewed, histogram of the lengths of the edges and the latency of the found CCEP responses. Figure 2.1 shows the highest peak of edge length to be around 20 millimeters in length, corresponding to the inter-electrode distance in all patients indicating mostly local responses between neighboring electrodes. The latency histogram in Figure 2.2 shows a similar graph, with most latencies being around 0.03 seconds with a few outliers present above 0.06 seconds.

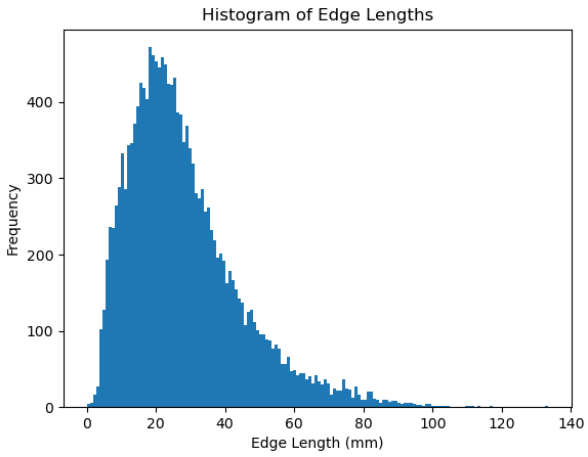

Figure 2.1: *Histogram of the distribution of edge lengths. No negative edge lengths can be seen and a distinct peak around 20mm in length is present.*

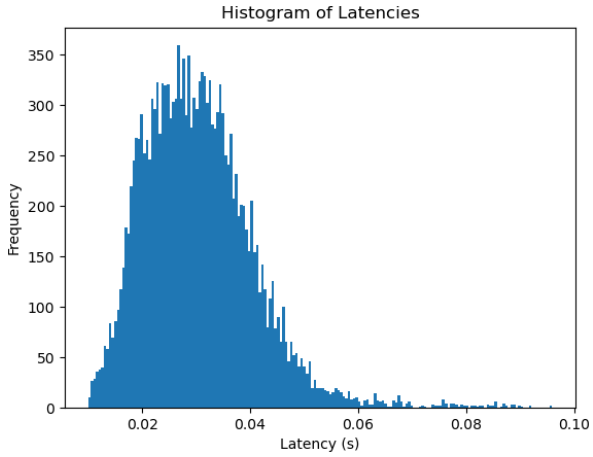

Figure 2.2: *Histogram of the distribution of latencies. No latencies below 0.009 seconds can be seen. A peak around 0.03 seconds is present.*

Figure 2.3 shows the scatterplot showing the relation between latency and edge length. Although the scatterplot shows a few outliers and a very broad distribution of both edge length and latency, a correlation with an R of 0.37 can be found between latency and edge length, showing a higher latency with increased edge length.

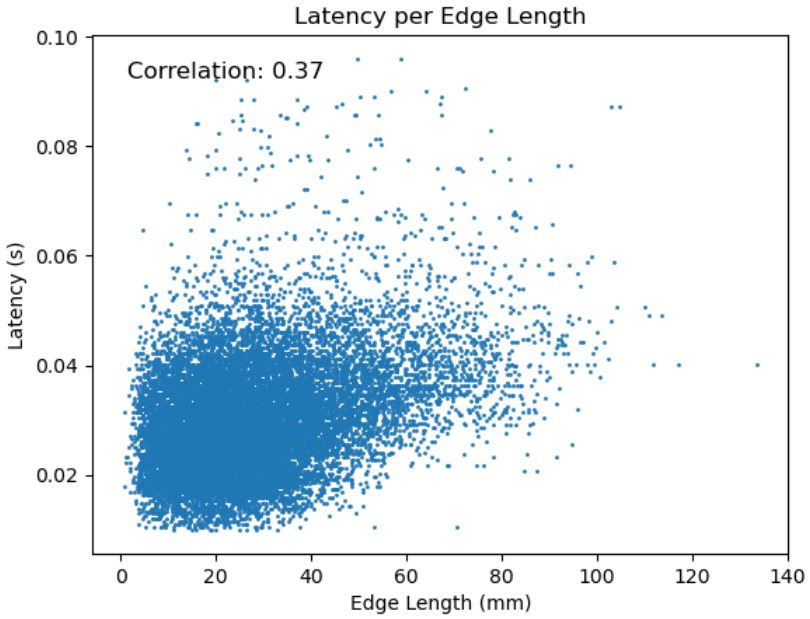

Figure 2.3: *Scatterplot of the latency per edge length. No negative edge lengths and latencies below 0.09 are present. A correlation of 0.37 is calculated on the scattered points.*

2.3.2 Destrieux Label Analysis

Grouping all electrodes with the same Destrieux label across all 74 patients allowed for the reduction of nodes in the connectivity graph to the number of used Destrieux labels. Figure 2.4 shows a side view of a 3D representation of the brain. In this example of Destrieux connectivity visualizations, the left side of the brain shows the nodes and edges of the connected brain regions. The nodes in this figure correspond to the average electrode position of all 74 patients per brain region, and the edges or lines between the nodes show the connections between these regions. The opacity of the line shows the weight of the connection, based on the percentage of CCEP responses per stimulated area.

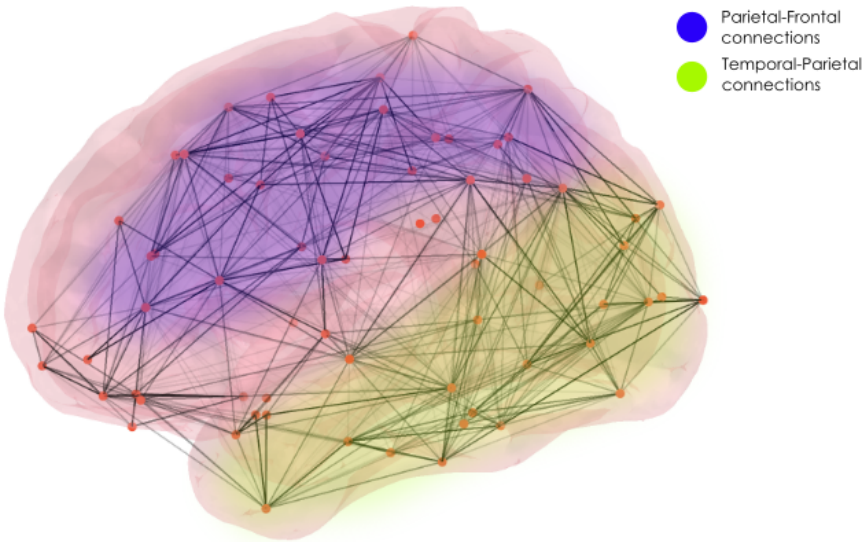

Figure 2.4: *3D representation of the left side of the brain with plotted connections between nodes based on Destrieux labels. Nodes in this figure correspond to the average electrode position of 74 patients per brain region. The opacity of the line shows the weight of the connection. Colored parts of the connections show the parietal-frontal, and temporal-parietal connections. Full 3D image is available on GitHub at:* `https://github.com/JeroenTeurlings/TM3_CCEP`.

In this example, a general view of global connectivity is visualized. Although most connections are only local connections, meaning neighbouring brain regions that react to stimulation of the other, some distant connections can be spotted. Although weaker than the local connections, distant connections show connections between temporal and partietal regions, as well as between parietal and frontal regions.

Full and interactable visualizations of the CCEP connections based on Destrieux labels are stored in a public GitHub repository accessible via: https://github.com/JeroenTeurlings/TM3_CCEP In this report, a single image with a single point of view is presented, aiming to capture the three-dimensional organization of connectivity in the image. It is recommended to view the full models on the GitHub page provided above, to gain full insight in the information stored within the data.

2.3.3 Individual Electrode Analysis

Analysis of the connections between individual electrodes provides more raw and unfiltered data compared to the Destrieux based connections as described above. Plotting all individual electrodes of the 74 included patients on a 3D representation of a brain shows a uniform distribution of the electrodes across the lobes of the brain, as can be seen in Figure 2.5. Electrode positions seem to follow the sulci of the brain, indicating that ECoG grids are placed on the surface of the brain, and are never inserted in the brain or folded in gyri. Frontopolar and occipital areas show the least amount of electrodes, corresponding with the less frequently operated on areas within the brain. The sylvian fissure, an anatomical separation between temporal and frontal lobes, can be seen due to the lack of electrodes in this area. With this distribution of electrodes, an accurate analysis can be performed.

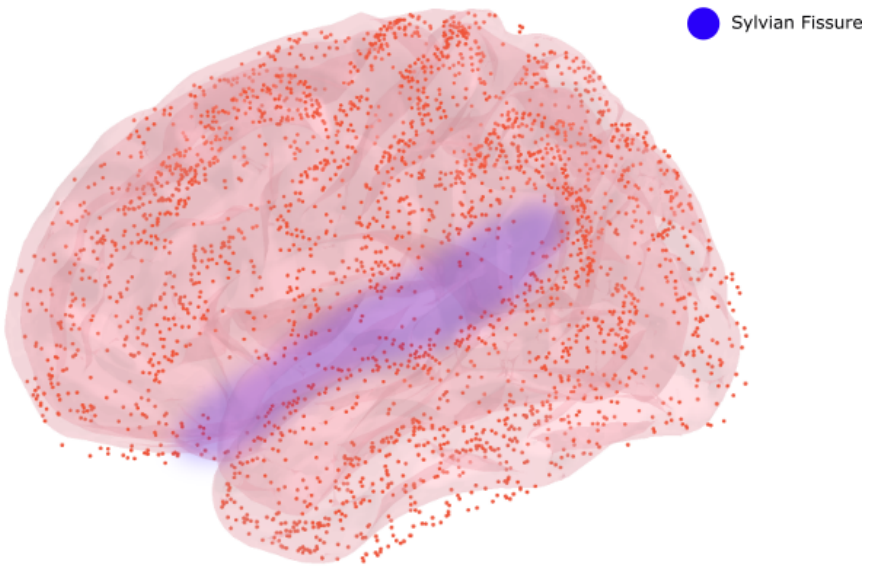

Figure 2.5: *3D representation of the brain with every individual electrode of the 74 patients visualized. A uniform distribution can be seen. The Sylvian fissure is highlighted and shows limited electrode placement.*

Adding all the connections between these electrodes shows an abundance of edges between the nodes, shown in Figure 2.6. This again shows the sylvian fissure acting as both an anatomical and signal separation between the frontal and temporal lobes. Additionally, most of the connections seen in this graph represent local responses, creating lines between neighboring nodes and flooding the image with edges.

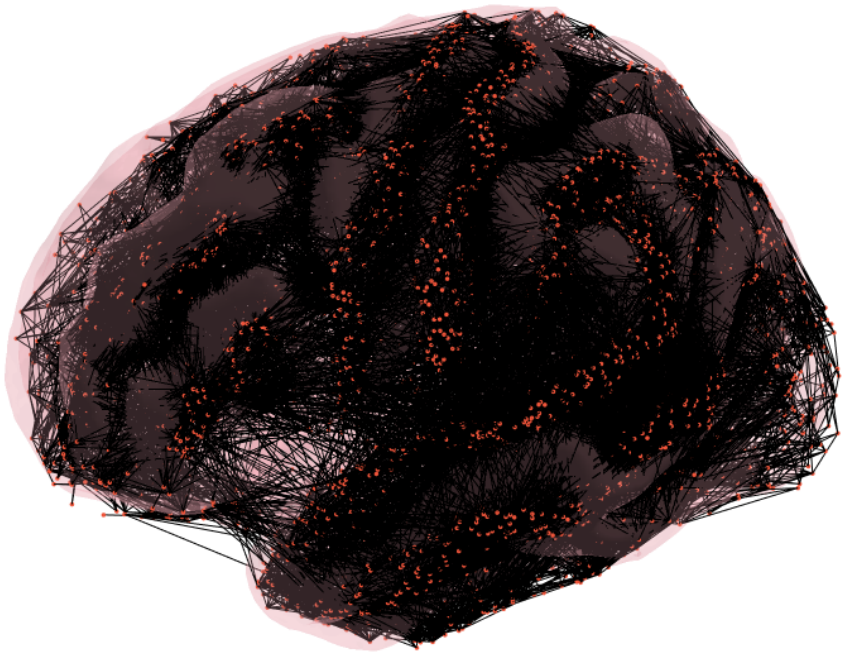

Figure 2.6: *3D representation of the brain with all the nodes and edges visualized. Due to the amount of local, neighboring connections, the image is flooded with edges. The beginning of the sylvian fissure can be seen, indicated by the lack of edges in the lower left corner of the brain visualization.*

After filtering out the edges that are shorter than 80 millimeters in length, the local responses are removed from the visualization, and only the distant connections remain. Figure 2.7 shows the same 3D visualization as before, but only with the edges that are long enough to be included in the analysis. This visualization shows significantly less edges than before. Two big bundles of connections can be extracted from this view, namely the connections between the temporal lobe and the parietal lobe, as well as the connections between the parietal lobe and the frontal lobe.

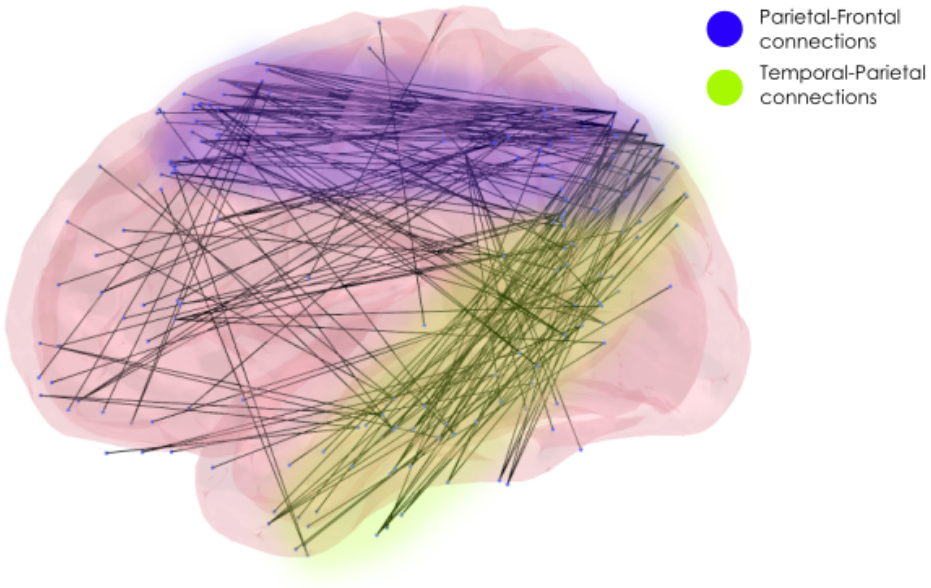

Figure 2.7: *3D visualization of the brain with all edges longer than 80 millimeters in length plotted. The bundles of temporal-parietal connections and parietal-frontal connections are highlighted.*

After applying weight to the edges, a more concise image emerges. Applying opacity to the lines based on latency (short latency/quick responses being fully opaque) and applying thickness of the line based on amplitudes (high amplitude responses being the thickest) gives the visualization presented in Figure 2.8. Here, the same two bundles of connections can be found as before, and connections outside these two bundles vanish by becoming less thick (lower amplitude) and less opaque (higher latency).

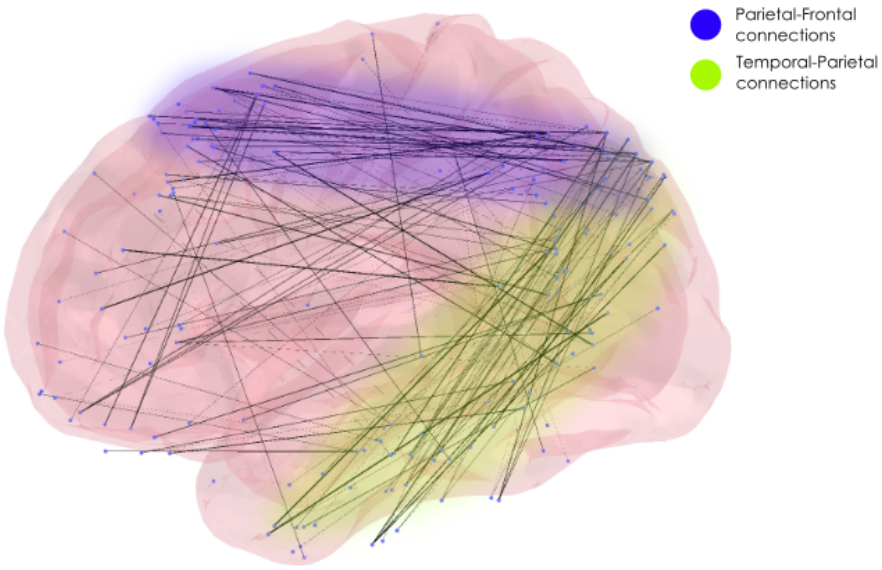

Figure 2.8: *3D visualization of the brain with all the edged longer than 80 millimeters in length, filtered on latency and amplitude. Opacity of the line is based on latency, and thickness of the line is based on amplitude. The bundles of temporal-parietal connections and parietal-frontal connections are highlighted.*

Again, full and interactable visualizations of the CCEP connections based on individual electrodes are stored in a public GitHub repository accessible via: `https://github.com/JeroenTeurlings/TM3_CCEP` It is highly recommended to view the full models on the GitHub page provided above.

2.3.4 Tract Comparison

In Figure 2.9, the white matter tracts found through DTI analysis as provided by the article by Van Blooijs et al. (2023) are shown [19]. These white matter tracts are based upon the same 74 patients that are analyzed in this thesis and show four distinct white matter tracts: the AF, SLF frontal-parietal, SLF frontal-central, and the TPAT. Comparing these tracts with the presented results of this study shows similarities between the SLF frontal-parietal and the TPAT white matter tracts, and the two bundles of electrode connections shown before.

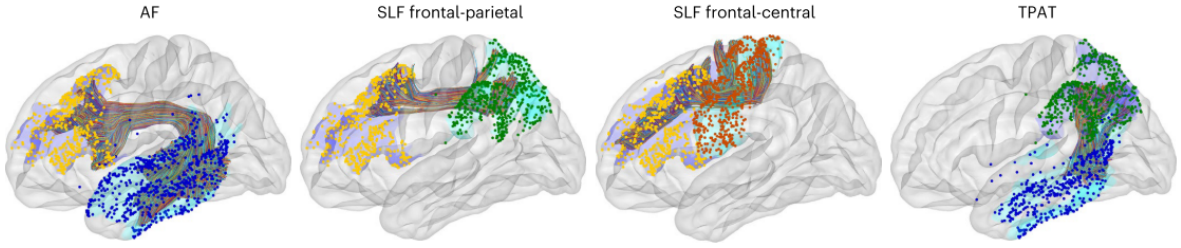

Figure 2.9: *3D visualizations of the brain showing different white matter tracts and electrode positions at endpoints from all 74 subjects used in this study. Adapted from Van Blooijs et al. (2023) [19]*

2.4 Discussion

2.4.1 Overview

This study successfully demonstrates the utility of CCEP in mapping brain connectivity, revealing patterns that align with known anatomical tracts. By utilizing both Destrieux label-based grouping and individual electrode analysis, this research shows patterns of local and distant neural interactions. Filtering on edge length and adding weights based on latency and amplitude improves found results and extracts potentially meaningful connections between brain areas. Furthermore, the comparison with white matter tracts derived from DTI offers a comprehensive view of the structural and functional connectivity, reinforcing the validity of the observed CCEP connections. This underlines the possibility of using CCEPs for connectivity based analysis as an alternative for standard DTI measurements, showing that we can find the same connections based on CCEP measurements. These results shed light on brain connectomics in this patient population.

2.4.2 Edge Length and Latency

The distribution of edge lengths and latencies of the CCEP responses shown in the histograms indicates predominantly local interactions. The peak edge length around 20 millimeters (similar to the interelectrode distance) suggests that most detected CCEP responses occur between adjacent electrodes, highlighting the sensitivity of the method to local brain dynamics. The observed correlation between edge length and latency, although slight, suggests that longer connections tend to have higher latencies. This relationship is consistent with the idea that longer neural pathways require more time for signal transmission.

2.4.3 Connection Analysis

Grouping electrodes by Destrieux labels allowed for a general and macro-level view of brain connectivity. The connectivity patterns revealed through this method indicate strong local interactions, with several distant connections between temporal, parietal, and frontal regions. The connection strength between the different brain regions revealed the following insights:

- **Connection Strength Distribution**: The calculated weights, indicating the percentage of stimulations that evoked responses, varied across different Destrieux regions. Higher weights were observed in regions traditionally associated with strong connectivity, such as temporal and parietal regions or parietal and frontal regions, whereas regions like temporal and frontal regions exhibited weaker connections.
- **Anatomical Separation**: The sylvian fissure, providing an anatomical separation between the temporal and frontal lobes, acts in this visualization also as a separation in signal connections. This can be concluded from the mirrored C-like shape of the connections, flowing from the temporal lobe over to the occipital and parietal lobes, before ending in the frontal lobe. Little to no connections are visible between the temporal and frontal lobes.

The analysis of individual electrode connections provided a more detailed view of the neural network, revealing a dense array of local connections. The reduction of this complexity by filtering out short edges emphasized the significance of distant connections, particularly between the temporal-parietal and parietal-frontal regions. Applying amplitude and latency characteristics to the remaining edges further improved and distilled the visualization of these two connection bundles. Although there are still plenty of other connections present in the visualization, the temporal-parietal and parietal frontal bundles stand out.

2.4.4 Tract Comparison

When comparing the white matter tracts from the study by Van Blooijs et al. (2023) [19] with the CCEP connections found in this study, some similarities arise. Mainly the SLF frontal-parietal and the TPAT white matter tracts show similarities with the two bundles of electrode connections shown before. This similarity hints at these two bundels of electrode CCEP connections being the same as

the TPAT and SLF frontal-parietal white matter tracts. Since the same cohort of patients is analyzed in both studies, it was expected to find similar results. However, it is of added value to see that the same white matter tracts can be found with CCEP analysis, instead of DTI imaging.

The comparison with DTI-derived white matter tracts offers validation for the functional connections observed through CCEP. The similarities between the SLF frontal-parietal and TPAT tracts and the identified CCEP bundles support the idea that these functional pathways are maintained by structural connections. This similarity between structural and functional data shows the reliability of CCEP as a tool for mapping brain connectivity. The consistency between CCEP-derived connectivity patterns and DTI-based tracts validates the use of CCEP for studying brain connectivity. This validation supports the continued use of CCEP in both clinical and research settings for mapping functional networks.

The dominance of local connections and the presence of significant long-range interactions provide insights into how the brain integrates and processes information. These connectivity patterns are essential for understanding normal brain function and the disruptions caused by neurological disorders. The detailed mapping of functional connections can inform surgical planning, especially in epilepsy surgery, where preserving critical functional pathways is crucial. The ability to visualize and quantify these connections can enhance the precision of surgical interventions. However, clinical translation to personal visualizations finetuned to specific patients is still needed.

2.4.5 Strengths and Limitations

The power of this analysis lies in its demonstration of an alternative method for visualizing brain connectivity. By using CCEPs, this study provides an alternative approach to DTI-based visualizations. CCEPs offer insights into functional connectivity that are more intuitive than analyzing individual electrode traces alone. While individual electrode traces contain valuable information, they are challenging to interpret. The method presented in this chapter simplifies this by providing a intuitive visualization of connections for an entire patient population. This overview can serve as a foundation for further research.

The connections identified through this analysis are documented in the 'total_data.tsv' file available on the project's GitHub page. This file allows replication of results and the development of new methods. Each row in the file represents a connection between two electrodes, including their Cartesian coordinates, Destrieux labels, and details such as amplitude and latency of the detected CCEP. Additionally, a label indicates whether the CCEP N1 peak is correctly identified (0) or incorrectly identified (1). This dataset is useful for training machine learning algorithms to improve CCEP recognition. The intuitive nature and availability of the data are significant strengths of this study and promotes the use of the data for further research.

Despite the valuable insights provided, this study has some limitations. Firstly, the findings are based on a specific patient cohort, and their generalizability to broader populations is uncertain. Future research should include more diverse patient groups to enhance the applicability of the results. Additionally, the current analysis offers a static view of brain connectivity, representing a specific moment in time, which may not be generalizable. It is crucial to consider patient dynamics when interpreting these results.

The comparison with known tracts from the article by Van Blooijs et al. (2023) indicated that while it was possible to extract both the TPAT and the SLF frontal-parietal tracts, other tracts were not identified using the proposed method. The exclusion of connections shorter than 80 millimeters may have contributed to this limitation. Adjusting the filtering criteria or employing more sophisticated analyses could potentially reveal these connections. However, the optimal lower bound for edge length remains unclear, as no formal validation of this parameter has been done beyond visual inspection. Investigating optimal cut-off values or alternative filtering methods can be useful.

Additionally, the visualized data remains noisy, with some connections not aligning with current knowledge of brain connectivity. This could indicate either the discovery of new, undocumented connections or the presence of non-significant CCEP responses. The peak detection algorithm, while designed to accurately detect CCEPs, is not fully accurate and introduces noise, complicating accurate analysis. The large amount of excluded CCEPs show the difficulty in finding accurate responses. Improvement of the peak detection algorithm is important, as this is a critical part of any CCEP study.

2.4.6 Future Recommendations

Given the accessibility of the data used in this study, future research can build upon the work presented in this chapter. A promising direction would be to delve deeper into Graph Analytics to explore features such as node centrality or clustering within the data. These advanced analytical methods can provide more detailed insights into the types of connections present in the brain and the network as a whole. While the results presented in this study are informative, they remain basic. Advanced filtering techniques, such as using Fréchet distances, could help visualize more complex connection bundles within the graph, potentially identifying the remaining white matter tracts as defined by Van Blooijs et al. (2023) [19] and uncovering currently unknown connections.

Another area for future exploration is dynamic functional connectivity, capturing how neural interactions evolve over time and in response to different cognitive tasks or stimuli. The current analysis offers a snapshot of brain connectivity based on CCEPs but is limited to a single moment in time. Patients in this study were measured while awake but not performing any notable tasks, providing a representation of resting state connectivity. Future research should compare CCEP measurements during resting states with those obtained during various cognitive tasks. This could offer a deeper understanding of brain dynamics and functional or effective connectivity.

Clinical translation of these findings is crucial. Understanding how brain connectivity knowledge can be used to diagnose or treat network diseases such as epilepsy remains largely unknown. Analyzing brain connectivity through CCEPs provides a novel approach that could improve our understanding of these disorders. Chapter 3 offers an initial step towards clinical translation by focusing on individual network analysis. Expanding the analysis to include general population brain connectivity can enhance our comprehension of brain disorders as a whole.

CHAPTER 3

Individual Connectivity Visualizations

3.1 Introduction

During brain surgery, the EOR of the tumor is associated with outcome after the procedure, as described in the chapter "Background" [6, 7, 8]. Therefore, it is crucial to accurately differentiate between tumorous and healthy tissue and between functional brain tissue and regions with less critical functionalities. This allows neurosurgeons to determine which parts of the brain can be safely removed and which parts must remain intact to preserve the patient's critical functions post-operatively.

Pre-operatively, fMRI and DTI are most commonly used to visualize anatomical structures and functional regions within the cortex [32]. These imaging modalities excel in visualizing important cortical areas and greatly assist neurosurgeons. However, a significant disadvantage is their unavailability in the OR once the procedure begins. Another disadvantage is that these techniques capture an image before the surgery starts, and cannot be updated during surgery. Once the skull is opened, the brain shifts, making it more difficult to fully depend on the pre-operatively made scans for navigation [33].

During surgery, Direct Electrical Stimulation (DES) is the gold standard for brain mapping, as an alternative for the pre-operatively used scans [34, 35]. This technique involves applying an electrical stimulus to the cortex and monitoring any functional loss in the patient, thus localizing eloquent tissue and enabling safe resection. During the testing, the patient is awake to document any changes in the body, which aids with mapping of the cortex. Additionally, every part of the cortex within the resection zone needs to be tested multiple times. Due to this, DES is time-consuming and uncomfortable for the patient.

Instead, ECoG combined with CCEP measurements could provide an alternative for intra-operative brain mapping. This technique allows for measuring underlying connected cortical areas without requiring the patient to be awake during surgery. This approach facilitates more accurate brain mapping without relying on DTI or other pre-operative imaging techniques [13]. CCEPs enable the precise measurement of connections between brain regions and the visualization of specific tracts within the brain. As demonstrated in Chapter 2, ECoG and CCEPs can record and can be used to visualize connectivity between brain regions. This capability could potentially translate into clinically useful measurements during surgery to visualize connections in individual patients.

ECoG can be used for both mapping and monitoring purposes [11, 36, 37, 38, 39]. ECoG can map specific brain areas similarly to DES if the patient is awake. When the patient is asleep, CCEPs can help locate regions tightly connected to other important areas, indicating critical regions within the cortex that should be avoided during surgery. By providing the same signal regularly during the OR session, any changes in signal propagation can be detected, and the neurosurgeon can be alerted. Additionally, with an ECoG grid in place, the patient can be continuously monitored for after discharges or epileptic seizures during surgery.

At Erasmus MC hospital, ECoG measurements are not yet routinely performed, and CCEPs have not been recorded. There is currently limited experience with CCEP and ECoG data analysis. Clinical translation of brain connectivity to individual application in the OR is needed. This chapter aims to present a new method of visualizing functional connectivity within the brain in a clear and intuitive way.

3.2 Methods

3.2.1 Electrode localization

During surgery, each patient has a unique placement of electrodes, as there is no standard placing montage within ECoG measurements. Therefore, it was crucial to localize the electrodes used for each patient. This was achieved by extracting the Cartesian coordinates of the electrode positions from the provided data files. A custom montage was created in MNE by defining the electrode positions in MNI152 space, which was consistent with the recorded electrode positions in the article by Van Blooijs et al. (2023) [19]. Once calibrated to a standard FreeSurfer fsaverage brain (a brain reconstruction made by averaging 40 unique healthy brain MRI scans [40]), a 3D visualization was generated, displaying the electrode positions for each patient.

3.2.2 Visualization of CCEP Amplitudes and Latencies

The amplitudes and latencies from the registered CCEPs, along with the raw timeseries data, were used to produce visualizations. Each electrode has its own signal trace from which a CCEP could potentially be registered. At the peak of the recorded CCEP, amplitude and latency were extracted. The values of these amplitudes and latencies could then be projected per electrode on there corresponding position on the brain.

For each stimulating electrode pair, the amplitudes of the registered CCEPs were normalized and assigned a varying intensity of red based on the amplitude. These colors were then projected on the corresponding electrodes. Higher amplitudes resulted in a more intense red color. Electrodes that did not register a CCEP were left white, while the stimulating electrodes were colored yellow for reference.

Similarly, the latencies of the registered CCEPs were normalized and assigned a varying intensity of blue based on latency. These colors were then also projected on the corresponding electrodes on a separate brain reconstruction. Lower latencies (quicker signal transmission) resulted in a more intense blue color. Electrodes that did not register a CCEP were left white, and the stimulating electrodes were colored yellow for reference.

3.2.3 Combined Amplitude and Latency Animation

Visualizations of both amplitude and latency were combined into an animation to assess the evolution in time of both parameters. Individual timeseries from the electrode traces were extracted to follow the potential of each electrode over time. Electrodes were colored blue (for negative potential) based on their amplitude to focus on the registered N1 peaks within the signal, creating a visual representation of the negative potential distribution across the electrodes at specific time points.

The analysis covered time points from -100ms to 200ms around the stimulus point, generating individual frames that were combined into an animation of amplitude distribution over time. To prevent extreme outliers from skewing the amplitude distribution, amplitudes were Winsorized, bringing the top 1% of amplitudes down to the rest of the dataset. Additionally, an option was added to binarize the colors: once a significant CCEP peak was detected, the electrode would turn bright blue or no color at all, focusing on the presence of a significant peak rather than the amplitude's height. In total, an animation was created with the brain representation on top, showing all the electrodes and their corresponding amplitude of the signal, and with a timeline of the raw electrode traces on the bottom, giving a total overview of the evolution of the recorded signals over time.

In this thesis, an example of one specific patient (patient 10) and one specific stimulation electrode pair (T33-T44) will be shown. Showing every patient and every electrode pair was deemed not feasible for this report, but results from these patients and stimulation electrode pairs can be reconstructed by using the open-source dataset provided by Van Blooijs et al. (2023) [19] and the Python script provided on the aforementioned GitHub page.

3.3 Results

3.3.1 Electrode Localization

Each patient's electrode placement is successfully localized and visualized on the 3D fsaverage brain. The custom montage created in MNI152 space allows accurate projection of electrode positions. The 3D visualizations reveal the unique electrode configurations for each patient, ensuring a reliable foundation for following analysis. An example of the visualization of electrode positions can be found in Figure 3.1. In this specific example of patient 10, you can see the electrodes are spaced throughout the temporal, frontal, parietal and occipital lobes of the brain. This allows for accurate representation of the situation within the OR, and gives an idea on which possible connections we can find in the covered areas.

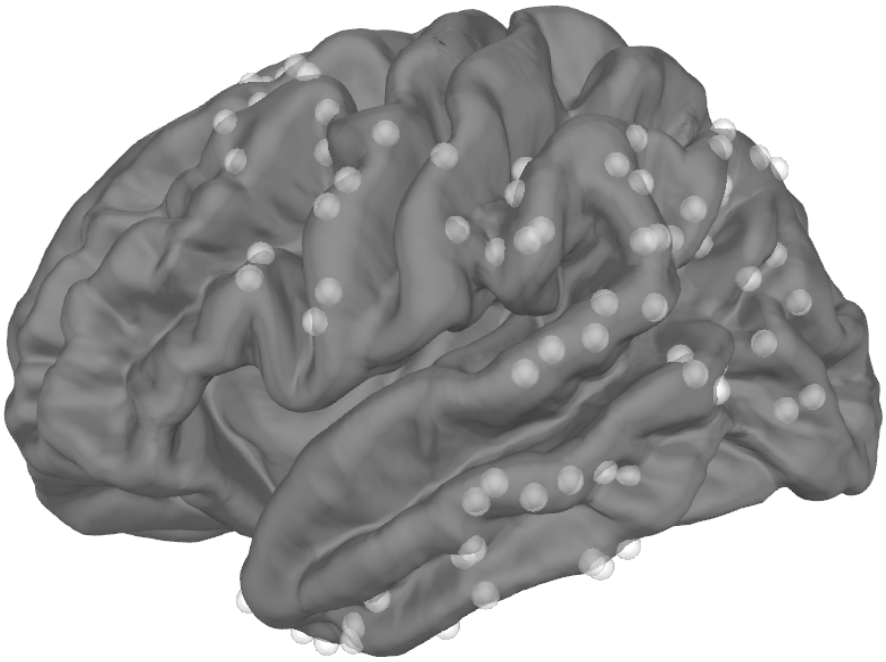

Figure 3.1: *3D representation of electrode distribution of patient 10. Light gray spheres represent electrodes as registered by an MRI scan. Electrode positions are morphed to the MNI152 space to fit this example brain.*

3.3.2 Visualization of CCEP Amplitudes

The visualization of the brain with its electrodes functions as the foundation for further visualizations. For each patient, the normalized amplitudes of the registered CCEPs are visualized on the 3D brain model. An example of the same patient as before can be seen in Figure 3.2. The intensity of the red color on the electrodes varied according to the amplitude of the registered CCEP response. The higher the amplitude, the more intense the red. Electrodes that did not register a CCEP are marked in white. The stimulating electrode pairs are yellow, serving as a reliable reference point and indicating the region that is being stimulated. This may hint to what possible connections could be present in these regions. In this specific example, local responses are present, indicated by the few red electrodes around the stimulation electrode, as well as a few distant connections. The red electrodes in the frontal and temporal lobes of the brain hint towards a connection between the stimulation area, and the two distinct reaction zones.

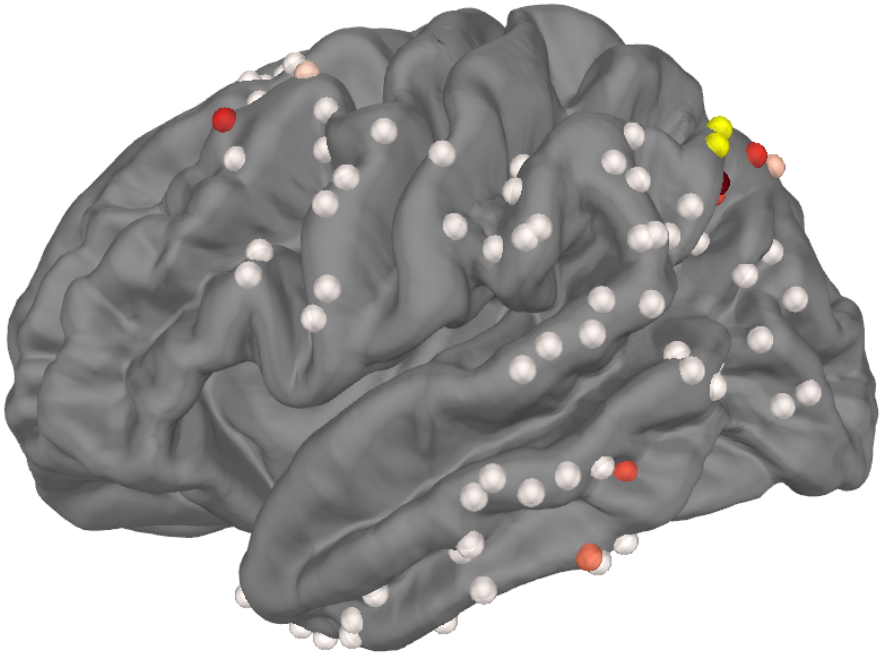

Figure 3.2: *3D representation of the brain with its electrodes of patient 10, stimulated on electrode T43-T44. Yellow electrodes indicate the stimulation electrodes. The amplitude of the response per electrode is shown in a hue of red. Apart from local responses around the stimulation electrodes, a distant response can be seen in the frontal and temporal regions.*

3.3.3 Visualization of CCEP Latencies

The normalized latencies of the registered CCEPs are visualized with varying intensities of blue. An example of the same patient as before can be seen in Figure 3.3. Electrodes with shorter latencies (indicating quicker signal transmission) displayed a more intense blue color. As with the amplitude visualization, electrodes that did not register a CCEP were left white, and the stimulating electrodes were colored yellow for reference. In this specific example of patient 10, faster responses were seen around the stimulation area and in the same distant areas where amplitude increases were found. This shows fast and strong reactions in the frontal and temporal regions when stimulating in the parietal region of this specific patient.

3.3.4 Combined Amplitude and Latency Animation

The combined animation, depicting both amplitude and latency over time, provide dynamic insights into brain activity during CCEP stimulation. The animation can be seen in snapshots of the whole animation on key timepoints in Figure 3.4. Here, only the negative potentials are depicted to focus on the N1 CCEP response. These potentials are portrayed in blue, and are binarized. Electrodes only turn completely blue when a CCEP is registered. Shown below the 3D visualizations of the brain are the raw signal traces of all the electrodes. Before stimulation, no response is registered. During stimulation, a large part of the brain is excited, corresponding with the large stimulus artefact shown below the image. Part of the electrodes become negative, and part become positive, corresponding with the polarity of the stimulation on the different electrodes. Some time after the stimulation, the local and distant regions of the brain light up, showing their registered CCEP response.

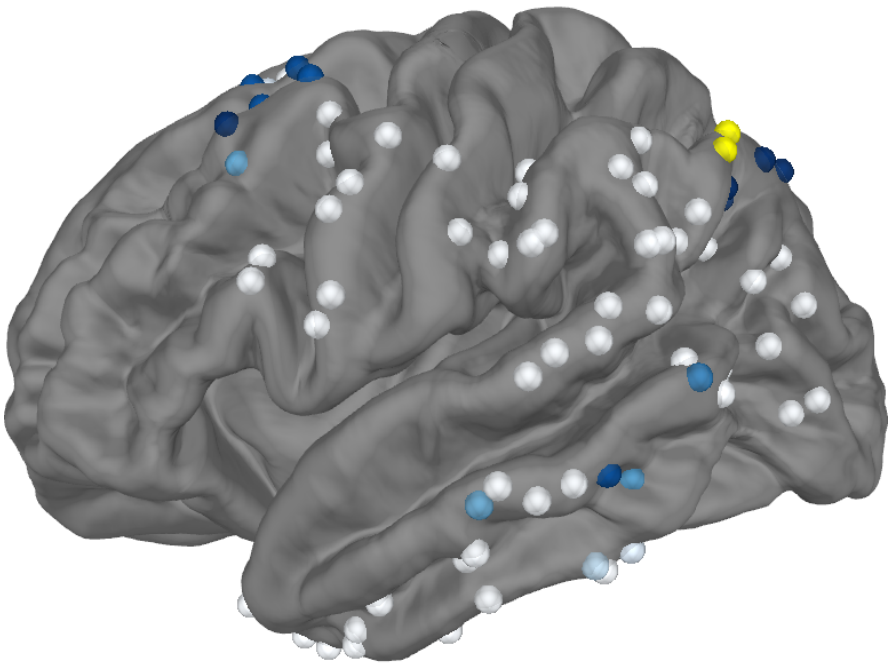

Figure 3.3: *3D representation of the brain with its electrodes of patient 10, stimulated on electrode T43-T44. Yellow electrodes indicate the stimulation electrodes. The latency of the response per electrode is shown in a hue of blue. Apart from fast local responses with a low latency, fast distant responses can be seen in the frontal and temporal regions.*

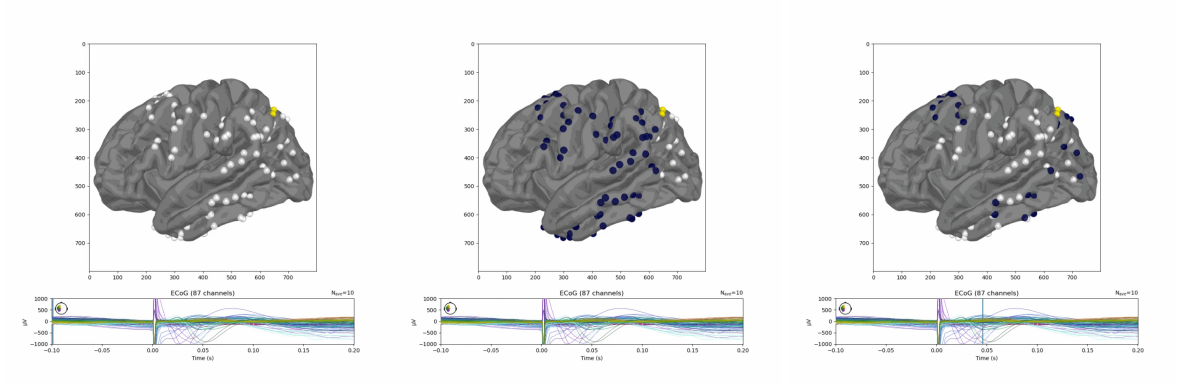

Figure 3.4: *Three different timepoints in the animation of the progression of the CCEPs of patient 10, stimulated on electrodes T43-T44. Blue electrodes show binarized negative CCEP responses. The stimulation electrodes are shown in yellow. Below each brain plot a timeline is plotted with all the raw electrode potentials shown. A vertical line shows the moment in time of the snapshot. From left to right: 1) 100 milliseconds before stimulation, no CCEP N1 peaks are detected, 2) the moment of stimulation (t=0), the stimulation creates a strong dipole stimulation artefact, showing blue electrodes left of the stimulation electrodes, 3) roughly 0.045 seconds after stimulation, showing local responses around the stimulation electrodes, and distant responses in frontal and temporal areas.*

Full animations of the CCEP signals (binarized amplitude animation and non-binarized animation) are stored in a public GitHub repository accessible via: https://github.com/JeroenTeurlings/TM3_CCEP. In this report, snapshots of the visualizations are presented, trying it's best to capture the dynamic present in the time bound animations produced by the analysis. It is recommend to watch the full animations on the GitHub page provided above, to gain full insight in the information stored within the data.

3.4 Discussion

3.4.1 Overview

This study aimed to show the patterns of brain connectivity through detailed visualizations of CCEPs in individual patients. By accurately localizing electrodes and visualizing CCEP amplitudes and latencies on 3D brain models, a comprehensive overview of the brain's functional responses to stimulation is provided. The combined animation of amplitude and latency further increased our understanding of the temporal dynamics of these responses. These findings underline the complexity and variability of brain connectivity and could have several implications for both clinical practice and future research.

Overall, the visualizations and animations revealed distinct patterns in CCEP responses across different patients, of which one example is shown. The localization and intensity of these responses varied between patients, underlining the individualized nature of brain activity. These findings contribute to a deeper understanding of neural connectivity and the efficacy of CCEP as a tool for mapping brain function.

3.4.2 Visualization of Amplitudes and Latencies

In the provided example, the red coloring around the stimulating electrodes indicated strong local responses, while the showing of red in distant electrodes suggested the presence of long-range connections. These findings show the possibility that within this patient, a functional tract is present between the parietal region around the stimulation electrodes, and the distant frontal and temporal areas. This is in line with the bundles of edges found in Chapter 2, and shows an example of registered white matter tract connection in this patient.

The latency visualizations, marked by varying intensities of blue, provided insights into the speed of signal transmission across different brain regions. The example showed faster responses (more intense blue) around the stimulation area and the distant connected regions, indicating rapid signal propagation. This pattern suggests efficient connectivity and shows that the connected regions not only propagate signals between each other, but also shows that this propagation is fast. The clear differentiation between areas of quick and delayed responses aids in understanding the temporal aspects of neural communication and may inform the identification of critical pathways for clinical interventions.

The combined animation of amplitude and latency over time offered a dynamic perspective on brain activity. Key observations included the temporal progression of CCEP responses, highlighting how brain activity evolves in response to stimulation. This dynamic visualization allowed for a clear distinction between active and inactive regions, enhancing the interpretability of the complex and abstract data for any neurosurgeon. The ability to visualize these changes over time is particularly valuable for understanding how different regions of the brain interact and respond to stimuli and how distant CCEP responses evolve over time, which is critical for both research and clinical applications.

3.4.3 Strengths and Limitations

One of the major strengths of this study is its ability to visualize connected brain regions in individual patients. By accurately localizing electrodes and visualizing CCEP amplitudes and latencies on 3D brain models, this study enables a comprehensive understanding of both the spatial and temporal dynamics of brain connectivity. These detailed visualizations provide clinicians and researchers with precise insights into brain function, which is crucial for informed decision-making in both clinical and research settings. Extending from the knowledge gained in the previous chapter, this reported method applies this to individual patients

The study focuses on producing intuitive and straightforward visualizations that can be utilized in the OR for clear visualization of connected areas within the brain. ECoG data, which contains a wealth of information, is often not easily interpretable when looking at raw signal traces. By translating this extensive data into clear visualizations, neurosurgeons and other clinicians can more effectively use the data from ECoG registrations to improve patient care and outcomes. During surgery, such visual-

izations can be useful in identifying connected areas within the brain, potentially aiding in improving treatment outcomes, although further research on this specific application is needed.

While this study provides valuable insights, some limitations should be addressed. Preprocessing and the labeling of electrodes as 'good' or 'bad' were performed by the original dataset authors, and the parameters for the peak detection algorithm were adopted from previous research without thorough verification. Although the algorithm produced mostly correct significant peaks, visual checks were still necessary to confirm CCEP responses. This reliance on manual verification indicates that the algorithm's specificity and sensitivity need improvement. Future work should prioritize refining the peak detection algorithm to reduce the need for visual checks and enhance its reliability.

A significant limitation is the generalization of anatomical data due to the morphing of electrode positions to the fsaverage brain space. Due to privacy concerns, individual MRI scans were not available, resulting in electrode positions that are approximate and may not accurately reflect precise anatomical locations. This generalization reduces the accuracy of visualizations and can impact the interpretability of observed connectivity patterns.

Most visualizations in the study focused on the amplitude of the CCEP response, an intuitive but potentially unstable parameter. The amplitude can be influenced by various factors, including electrode impedance, interference from non-neuronal sources, and the neutrality of the reference electrode. These factors introduce variability that may not accurately reflect the true strength of the neural response. Consequently, analyses based on amplitude should be interpreted with caution, and future research should consider more robust measures of neural activity.

3.4.4 Future Directions

A future goal of this project is the implementation of live CCEP analysis in the OR. This technique would allow for real-time monitoring and mapping of brain functionalities using ECoG and CCEP measurements, which is not yet routinely performed. Real-time visualizations could provide neurosurgeons with immediate feedback during surgeries, enhancing their ability to preserve critical brain functions. This project is a first step in realizing the use of ECoG and CCEP use in the OR, but further development and optimization of the proposed methods are needed. With this current system, the analysis of CCEPs can only be performed offline, and takes some time to complete. Before implementing this technique in the OR, speed and reliability needs to be improved.

However, the detailed mapping of CCEP responses can already significantly aid in pre-surgical planning, where online analysis is not needed. This can be useful for patients undergoing epilepsy surgery or other neurosurgical procedures like tumor resection. Understanding individual connectivity patterns can help preserve critical functional areas and improve surgical outcomes. Implementing a CCEP analysis in the pre-operative workflow is far from being realized in the Erasmus MC hospital, but further developmental steps can be made with the proposed methods.

Conclusions

This study aimed to map and analyze brain connectivity through detailed visualization of CCEPs in a cohort of patients. The research utilized techniques to visualize 3D brain reconstructions, visualize CCEP amplitudes and latencies, and compare functional connectivity with structural pathways derived from DTI. This study successfully demonstrated the utility of CCEP in mapping functional brain connectivity and highlighted the importance of integrating structural and functional data. The detailed visualizations of CCEP amplitudes and latencies, combined with comparisons to DTI-derived tracts, provided a robust framework for understanding brain connectivity. These findings have significant implications for clinical practice and neuroscience research, paving the way for more detailed, dynamic, and personalized analyses of brain connectivity. The methodologies and insights gained from this study represent valuable contributions to the field of neuroimaging and will inform future research and clinical applications. By providing insights on both general population-based brain connectivity, as well as visualizing individual connected brain regions, the study strenghtens the knowledge and the know-how of ECoG and CCEP analysis. Intuitively visualizing distant connections paves the way to further development of a implementing CCEP visualizations in the OR.

Key points of this study include:

- It is possible to reconstruct the connections between brain areas based on CCEPs instead of standard DTI imaging.
- There is a strong correspondence between functional CCEP pathways and known anatomical structures as demonstrated with DTI-derived white matter tracts, particularly in the temporal-parietal and parietal-frontal connections.
- Distant connected brain regions in individual patients can be registered and shown in easily interpretable visualizations.
- Combined animations of amplitude and latency can be used as a starting point for further personalized visualization of functional connectivity, especially for temporal progression and spatial distribution of CCEP responses.

In this master's thesis a method was developed for visualizing CCEP measurements in multiple ways. The results from this study can be used for further research in brain connectomics, as well as clinical application for the treatment of network-based brain disorders.

Bibliography

[1] Blumenfeld H. Neuroanatomy through clinical cases. Second edition ed. Sunderland, Mass. : Sinauer Associates; 2010. Available from: https://search.library.wisc.edu/catalog/9910206372202121.

[2] Buzsáki G, Anastassiou CA, Koch C. The origin of extracellular fields and currents-EEG, ECoG, LFP and spikes. Nature Reviews Neuroscience. 2012 6;13(6):407-20.

[3] Stone JL, Hughes JR. Early History of Electroencephalography and Establishment of the American Clinical Neurophysiology Society. J Clin Neurophysiol. 2013 2;30(1):28-44.

[4] Seidel S, Wehner T, Miller D, Wellmer J, Schlegel U, Grönheit W. Brain tumor related epilepsy: pathophysiological approaches and rational management of antiseizure medication. Neurological Research and Practice. 2022 12;4(1).

[5] Rasheed S, Rehman K, Akash MSH. An insight into the risk factors of brain tumors and their therapeutic interventions. Biomedicine and Pharmacotherapy. 2021 11;143.

[6] Vakani R, Nair DR. Electrocorticography and functional mapping. In: Handbook of Clinical Neurology. vol. 160. Elsevier B.V.; 2019. p. 313-27.

[7] Hervey-Jumper SL, Berger MS. Maximizing safe resection of low- and high-grade glioma. Journal of Neuro-Oncology. 2016 11;130(2):269-82.

[8] Sanai N, Polley MY, McDermott MW, Parsa AT, Berger MS. An extent of resection threshold for newly diagnosed glioblastomas: Clinical article. Journal of Neurosurgery JNS. 2011;115(1):3-8. Available from: https://thejns.org/view/journals/j-neurosurg/115/1/article-p3.xml.

[9] Kilbride RD. Intraoperative Functional Cortical Mapping of Language. J Clin Neurophysiol. 2013 12;30(6):591-6.

[10] Ghatol D, Widrich J. Intraoperative Neurophysiological Monitoring. Treasure Island (FL): StatPearls Publishing; 2023. Available from: https://www-ncbi-nlm-nih-gov.tudelft.idm.oclc.org/books/NBK563203/.

[11] Cordella R, Acerbi F, Broggi M, Vailati D, Nazzi V, Schiariti M, et al. Intraoperative neurophysiological monitoring of the cortico-spinal tract in image-guided mini-invasive neurosurgery. Clinical Neurophysiology. 2013 6;124(6):1244-54.

[12] Lang EW, Tomé AM, Keck IR, Górriz-Sáez JM, Puntonet CG. Brain connectivity analysis: A short survey. Computational Intelligence and Neuroscience. 2012;2012.

[13] Matsumoto R, Nair DR, LaPresto E, Najm I, Bingaman W, Shibasaki H, et al. Functional connectivity in the human language system: A cortico-cortical evoked potential study. Brain. 2004 10;127(10):2316-30.

[14] Bykanov AE, Pitskhelauri DI, Titov OY, Lin MC, Gulaev EV, Ogurtsova AA, et al. Broca's area intraoperative mapping with cortico-cortical evoked potentials. Zhurnal Voprosy Nejrokhirurgii Imeni NN Burdenko. 2020;84(6):49-56.

[15] Boyer A, Ramdani S, Duffau H, Dali M, Vincent MA, Mandonnet E, et al. Electrophysiological Mapping During Brain Tumor Surgery: Recording Cortical Potentials Evoked Locally, Subcortically and Remotely by Electrical Stimulation to Assess the Brain Connectivity On-line. Brain Topography. 2021 3;34(2):221-33.

[16] Tamura Y, Ogawa H, Kapeller C, Prueckl R, Takeuchi F, Anei R, et al. Passive language mapping combining real-time oscillation analysis with cortico-cortical evoked potentials for awake craniotomy. Journal of Neurosurgery. 2016 12;125(6):1578-9.

[17] Mandonnet E, Vincent M, Valero-Cabré A, Facque V, Barberis M, Bonnetblanc F, et al. Network-level causal analysis of set-shifting during trail making test part B: A multimodal analysis of a glioma surgery case. Cortex. 2020 11;132:238-49.

[18] Gramfort A, Luessi M, Larson E, Engemann DA, Strohmeier D, Brodbeck C, et al. MEG and EEG data analysis with MNE-Python. Frontiers in Neuroscience. 2013;7.

[19] van Blooijs D, van den Boom MA, van der Aar JF, Huiskamp GM, Castegnaro G, Demuru M, et al. Developmental trajectory of transmission speed in the human brain. Nature Neuroscience. 2023 4;26(4):537-41. Available from: https://www.nature.com/articles/s41593-023-01272-0.

[20] Demuru M, van Blooijs D, Zweiphenning W, Hermes D, Leijten F, Zijlmans M. A Practical Workflow for Organizing Clinical Intraoperative and Long-term iEEG Data in BIDS. Neuroinformatics. 2022 7;20(3):727-36.

[21] Holdgraf C, Appelhoff S, Bickel S, Bouchard K, D'Ambrosio S, David O, et al. iEEG-BIDS, extending the Brain Imaging Data Structure specification to human intracranial electrophysiology. Scientific Data. 2019 12;6(1).

[22] Fonov V, Evans A, McKinstry R, Almli C, Collins D. Unbiased nonlinear average age-appropriate brain templates from birth to adulthood. NeuroImage. 2009 7;47:S102.

[23] Destrieux C, Fischl B, Dale A, Halgren E. Automatic parcellation of human cortical gyri and sulci using standard anatomical nomenclature. NeuroImage. 2010 10;53(1):1-15.

[24] Sporns O, Tononi G, Kötter R. The human connectome: A structural description of the human brain. PLoS Computational Biology. 2005;1(4):0245-51.

[25] Bullmore E, Sporns O. Complex brain networks: graph theoretical analysis of structural and functional systems. Nature Reviews Neuroscience. 2009;10(3):186-98. Available from: https://doi.org/10.1038/nrn2575.

[26] Cao J, Zhao Y, Shan X, Wei Hl, Guo Y, Chen L, et al. Brain functional and effective connectivity based on electroencephalography recordings: A review. Human Brain Mapping. 2022 2;43(2):860-79.

[27] Hagmann P, Cammoun L, Gigandet X, Meuli R, Honey CJ, Van Wedeen J, et al. Mapping the structural core of human cerebral cortex. PLoS Biology. 2008 7;6(7):1479-93.

[28] Mori S, Zhang J. Principles of Diffusion Tensor Imaging and Its Applications to Basic Neuroscience Research. Neuron. 2006 9;51(5):527-39.

[29] Tagliazucchi E, von Wegner F, Morzelewski A, Brodbeck V, Laufs H. Dynamic BOLD functional connectivity in humans and its electrophysiological correlates. Frontiers in Human Neuroscience. 2012 12;6.

[30] Friston KJ. Functional and Effective Connectivity: A Review. Brain Connectivity. 2011;1(1):13-36.

[31] Sporns O. Graph theory methods: Applications in brain networks. Dialogues in Clinical Neuroscience. 2018;20(2):111-20.

[32] Lazar MS, Salamat AL, Alexander BJ, Jellison AS, Field J, Medow M. Tract Anatomy, and Tumor Imaging Patterns Matter: A Pictorial Review of Physics, Fiber Diffusion Tensor Imaging of Cerebral White. AM J Neuroradiol. 2004;25(3):356-69. Available from: http://www.ajnr.org/content/25/3/356.

[33] Nimsky C, Ganslandt O, Hastreiter P, Fahlbusch R. Intraoperative Compensation for Brain Shift. Surg Neurol. 2001:357-65.

[34] Sanai N, Berger MS. Evolution of Cortical Mapping Strategies. Neurosurg Focus. 2010;28.

[35] Duffau H, Capelle L, Sichez N, Denvil D, Lopes M, Sichez JP, et al. Intraoperative mapping of the subcortical language pathways using direct stimulations An anatomo-functional study. Brain. 2002;125:199-214.

[36] Herta J, Winter F, Pataraia E, Feucht M, Czech T, Porsche B, et al. Awake brain surgery for language mapping in pediatric patients: a single-center experience. Journal of Neurosurgery: Pediatrics. 2022 6;29(6):700-10.

[37] Saito T, Muragaki Y, Tamura M, Maruyama T, Nitta M, Tsuzuki S, et al. Monitoring Cortico-cortical Evoked Potentials Using Only Two 6-strand Strip Electrodes for Gliomas Extending to the Dominant Side of Frontal Operculum During One-step Tumor Removal Surgery. World Neurosurgery. 2022.

[38] Mohammadi AM, Sullivan TB, Barnett GH, Recinos V, Angelov L, Kamian K, et al. Use of high-field intraoperative magnetic resonance imaging to enhance the extent of resection of enhancing and nonenhancing gliomas. Neurosurgery. 2014;74(4):339-48.

[39] Ogawa H, Kamada K, Kapeller C, Hiroshima S, Prueckl R, Guger C. Rapid and minimum invasive functional brain mapping by real-time visualization of high gamma activity during awake craniotomy. World Neurosurgery. 2014 11;82(5):1-912.

[40] Fischl B, Sereno MI, Tootell RBH, Dale AM. High-resolution intersubject averaging and a coordinate system for the cortical surface. Human Brain Mapping. 1999;8(4):272-84.

Supplementary Material A

Table 1: *Overview of the included patients from the study by Van Blooijs et al. [19]. Sex, age, covered hemisphere and covered brain areas are documented.*

Sub-ccepAgeUMCU	sex	age	hemisphere	Frontal	Parietal	Occipital	Temporal
1	m	15	left	x	x	x	x
2	f	35	left	x			x
3	m	25	left	x	x		
4	m	4	right	x	x	x	x
5	f	17	right		x	x	x
6	m	26	right	x	x		
7	f	10	left			x	x
8	f	9	right			x	
9	m	21	left	x	x	x	x
10	m	15	left	x	x		x
11	m	5	left	x			
12	m	14	right	x			x
13	m	45	left	x			x
14	f	10	left	x			
15	m	15	right			x	x
16	f	42	left		x	x	x
17	m	4	both		x		
18	f	15	left	x			x
19	f	25	left		x		x
20	m	11	left	x			
21	f	12	right		x		
22	f	9	left	x			x
23	f	14	right	x			
24	m	17	right	x			x
25	m	16	right	x		x	x
26	m	7	right	x			
27	m	49	left	x			x
28	m	11	right	x			x
29	m	13	left		x		
30	f	14	left	x			
31	f	41	left	x			x
32	f	8	left	x			x
33	m	18	left	x	x		
34	f	7	left		x		
35	f	22	right				x
36	m	8	left	x	x		
37	m	28	left	x	x		
38	m	21	left	x		x	
39	m	14	left	x			
40	f	42	left	x			x
41	m	34	left				x
42	m	17	right			x	x
43	f	18	left	x	x		x
44	f	34	right		x		
45	m	22	left	x	x		x
46	f	36	left	x			x

Continuation of Table 1							
Sub-ccepAgeUMCU	sex	age	hemisphere	Frontal	Parietal	Occipital	Temporal
47	f	30	left			x	x
48	f	18	right	x			x
49	m	14	left		x		
50	m	7	left		x		
51	m	17	left		x		
52	m	44	left	x			
53	f	26	right	x			x
54	f	9	left	x	x		
55	m	14	right	x			
56	f	30	right				x
57	f	30	left			x	x
58	f	15	left		x	x	x
59	f	50	right	x			
60	m	15	right			x	x
61	f	5	left	x	x		x
62	m	8	left	x			x
63	f	33	left	x			x
64	m	36	left	x	x		
65	f	17	left	x			x
66	m	35	left	x	x		x
67	f	6	right	x	x		x
68	f	6	left	x			
69	f	51	left			x	x
70	f	38	right	x	x		
71	f	21	right	x	x		
72	f	27	left				x
73	m	23	right	x	x		
74	f	50	left	x	x		x